PHYSOR 2004 -The Physics of Fuel Cycles and Advanced Nuclear Systems: Global Developments
Chicago, Illinois, April 25-29, 2004, on CD-ROM, American Nuclear Society, Lagrange Park, IL. (2004)

Impact of Heterogeneous Cm-distribution on Proton Source Efficiency in Accelerator-driven Systems

Per Seltborg*, Jan Wallenius, Waclaw Gudowski
Department of Nuclear and Reactor Physics
Royal Institute of Technology, Stockholm, Sweden

The proton source efficiency (ψ^*) was studied for homogeneous and heterogeneous distributions of minor actinides in a nitride-fuelled and lead-bismuth-cooled accelerator-driven system. The findings from the MCNPX simulations indicate that, compared to a homogeneous configuration, a gain in ψ^* by up to 16% can be obtained by distributing the minor actinides heterogeneously, Cm being placed in the inner zone of the active core and Am in the outer zone. The reason for this is the higher fission probability for neutrons for Cm than for Am in the energy range below 1.0 MeV.

Moreover, a comparative study of two different physics packages available in MCNPX, the Bertini and the CEM models, has been performed, focusing on the production of neutrons in the spallation target and on the proton source efficiency. The Bertini model was found to produce a higher number of neutrons in the low-energy range (below ~15 MeV) than the CEM model. Consequently, the Bertini model also over-estimates ψ^* by about 10%, compared to the CEM model.

KEYWORDS: Proton source efficiency, Spallation, ADS, Transmutation, MCNPX, CEM, Bertini, Curium

1 Introduction

In accelerator-driven systems (ADS) [1-3], a sub-critical core is coupled to a high-power proton accelerator. The high-energy protons impinge on a target of heavy metal, generating a large number of neutrons via spallation reactions. The produced spallation neutrons leak out from the target, thus providing the surrounding sub-critical core with a strong external neutron source.

One of the objectives when designing an ADS is to try to attain as high power as possible to be produced in the core (yielding high transmutation rates), using as low proton beam power as possible. Since the construction of a reliable high-power proton accelerator is a difficult technical task and its operation is very expensive, the optimization of the efficiency of the source protons could have an important impact on the overall design of a future ADS and on the economy of its operation. In order to study the beam power amplification (core power divided by proton beam power) of an ADS, a new parameter, the proton source efficiency (ψ^*), was introduced in a previous study [4]. ψ^* represents the average importance of the external proton source, relative to the average importance of the eigenmode neutron production. It is defined in analogy with the neutron source efficiency φ^*, but relates the core power to the source protons instead of to the source neutrons. φ^* is commonly used in the physics of sub-critical systems, driven by any external neutron source (spallation source,

* Corresponding author, Tel. +46-8 55 37 82 04, E-mail: per@neutron.kth.se

(d,d), (d,t), ^{252}Cf spontaneous fission etc.). ψ*, on the other hand, has been defined only for ADS studies, where the system is driven by a proton-induced spallation source. The main advantages with using ψ* instead of φ* are that the way of defining the external source is unique and that ψ* is proportional to the beam power amplification. It has been shown that the source efficiency can vary considerably for different reactor cores. Studying ψ* for various system parameters is therefore of interest when designing an ADS.

The proton source efficiency is equal to the product of φ* and the number of source neutrons generated per source proton (Z_{tot}). We thus have the following relation between the *proton* source efficiency ψ* and the *neutron* source efficiency φ*;

$$\psi^* = \varphi^* \cdot Z_{tot} \ . \qquad (1)$$

For a fixed system (constant Z_{tot}), it follows that ψ* is proportional to φ*. However, when studying a change in a system design, Z_{tot} might also change and only ψ* remains proportional to the beam power amplification. ψ* could also, in analogy with the definition of φ* [5], be expressed in terms of k_{eff} and the total number of neutrons produced by fission in the core, for each source proton;

$$\psi^* = \left(\frac{1}{k_{eff}} - 1 \right) \cdot \frac{< \boldsymbol{F}\phi_s >}{< S_p >} \ . \qquad (2)$$

$<\boldsymbol{F}\phi_s>/<S_p>$ is the total production of neutrons by fission over the total number of source protons. Since $<\boldsymbol{F}\phi_s>$ is approximately proportional to the total power produced in the core, ψ* thus relates the core power directly to the proton beam intensity.

In the present paper, the proton source efficiency has been investigated for two different core configurations, the first with the minor actinides homogeneously mixed with each other and the second with the fuel heterogeneously distributed, curium being moved to the inner part of the core and americium to the outer part. In Section 2, the model used in the simulations is described and in Section 3.1, these two configurations are studied and compared for different radii of the spallation target. Section 3.2 describes a comparative study of two different physics packages provided by MCNPX [6], the Bertini model [7] and the Cascade-Exciton Model (CEM) [8].

2 System Modeling

Numerical simulations have been performed with the high-energy Monte Carlo code MCNPX in order to study ψ* for two different double-zone core configurations. In the first configuration, americium and curium were distributed homogeneously together with plutonium over the entire core, while in the second one, all of the curium was concentrated to the inner zone and the americium to the outer zone. A homogenized model of a uranium-free nitride-fuelled and lead-bismuth-cooled ADS was used and the composition of actinides in the fuel is based on the indefinite recycling of plutonium (40%), americium (51%) and curium (9%) in the second stratum of the double-strata fuel cycle strategy [9]. The actinide vector used in the model is listed in Table 1.

The simulations were performed for different target radii, varying from 10 cm to 50 cm. In the model depicted in Fig. 1, the target radius is 20 cm, which is also the inner boundary of the active core. The outer radius of the active core is in this case 70 cm and the height of it

Table 1 Relative fraction of actinides in the fuel

Plutonium	40%	Americium	51%	Curium	9%
Pu-238	5 %	Am-241	67 %	Cm-244	90%
Pu-239	38 %	Am-243	33 %	Cm-245	10%
Pu-240	30 %				
Pu-241	13 %				
Pu-242	14 %				

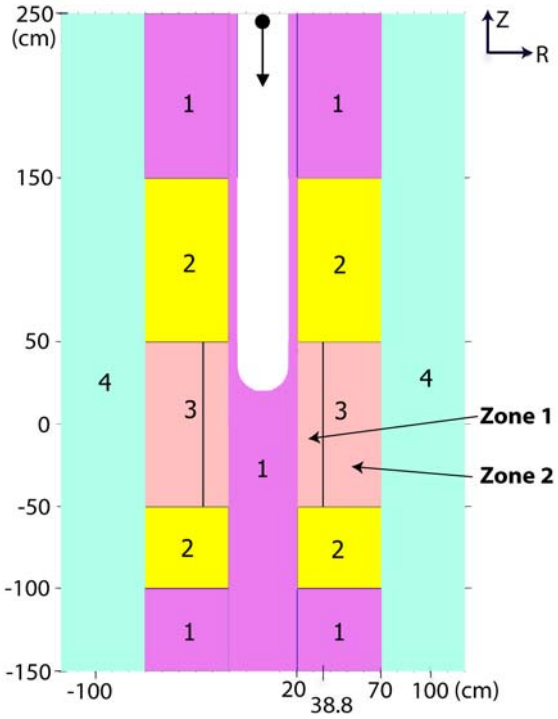

Fig. 1. RZ-view of the simulated model with target radius of 20 cm. The 1000 MeV protons are guided through the accelerator tube and impinge on the Pb-Bi spallation target. The different regions in the model are pure Pb-Bi (1), the plena (2), the active core (3) (zone 1 and zone 2) and the reflector (4).

100 cm. As the radius of the spallation target is varying, the outer radius of the core also needs to be changed, in order to maintain a constant reactivity and approximately the same volume of the core. The nitride fuel is mixed with an inert matrix of ZrN, and the fractions of inert matrix in the two zones were adjusted in order to obtain a k_{eff} of about 0.95 and to obtain the same maximum power density in the two zones, thereby yielding a flattening of the core power profile. In the heterogeneous configuration, the fraction of Pu was fixed to 40% in both zones, the fraction of Cm in zone 1 thus being 60%. The volume fractions of inert matrix in the different core zones are listed in Table 2. Due to the higher fission probability and fission neutron yield of Cm than of Am, the fraction of inert matrix in zone 1 is higher when Cm is concentrated to the inner zone of the core (75%), compared to when the minor actinides are mixed with each other (70%). The radius of the boundary between zone 1 and zone 2 was for each target radius determined by the matrix fractions and the total relative fractions of

actinides in the fuel. For the 20 cm target radius, the boundary was located at a radius of 38.8 cm.

Table 2 Volume fraction of inert matrix for the different core zones

Core configuration	Volume fraction of inert matrix	
	Zone 1	Zone 2
Homogeneous (Am and Cm mixed)	70%	66%
Heterogeneous (Am and Cm separated)	75%	64%

A 1000 MeV mono-energetic proton beam characterized by a Gaussian spatial distribution with a full width half maximum of 7.5 cm was used in the simulations. This proton source was guided through the vacuum beam tube of radius 15 cm towards the spallation target made of lead-bismuth eutectic. The Monte Carlo code MCNPX (version 2.3.0), in coupled neutron and proton mode, was used for all simulations, relying on the evaluated nuclear data library ENDF/B-VI.8. The high-energy physics package used by MCNPX was the Cascade-Exciton Model (CEM97).

3 Results and Discussion

3.1 Proton Source Efficiency for Homogeneous and Heterogeneous Cm Distribution

The main goal of this paper has been to investigate the impact on proton source efficiency of a heterogeneous distribution of Cm (zone 1) and Am (zone 2), compared to a homogeneous fuel distribution. From the results of the simulations, displayed in Fig. 2, we can draw the following conclusions. First, ψ^* decreases considerably when the radius of the spallation target increases. These results are in good agreement with our previous studies of the proton source efficiency [4, 10]. One reason for this behavior is the spectrum softening of the neutrons entering into the active core when the target is enlarged, since the probability to induce fission for neutrons strongly decreases with decreasing energy. The other main reason for the decrease in ψ^* is that the axial target neutron leakage increases with increasing target radius.

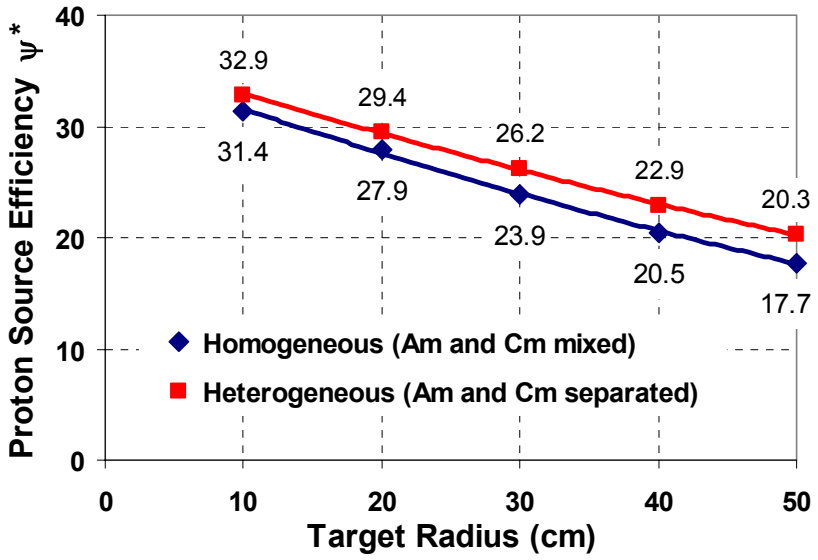

Fig. 2. Proton source efficiency ψ^* for different target radii of the homogeneous and the heterogeneous configurations (1σ-error ~0.50%).

Second, it is seen in Fig. 2 that, heterogenizing the fuel distribution by moving Cm to the inner zone and Am to the outer zone, increases ψ*, compared to when the two materials are homogeneously mixed with each other. The explanation for this is the higher fission probability for Cm than for Am, mainly in the energy range below 1 MeV, which is shown in Fig. 3. When the source neutrons leak out from the target and enter into the fuel, the first fission multiplication, normally occurring in the inner part of the core, is a determining factor for the magnitude of ψ*. Since a large fraction of the target leakage neutrons have energies below 1 MeV, the larger fission probability for Cm directly enhances the neutron multiplication and therefore increases ψ*. The gain in ψ* by concentrating Cm to zone 1 is further amplified for large target radii, as the spectrum of the neutrons entering into the fuel is softer in these cases. The fractions of target leakage neutrons below 1 MeV for the different target radii are listed in Table 3. The relative increase in ψ* by replacing the homogeneous fuel distribution by the heterogeneous distribution ranges from ~5% for the target radius of 10 cm to ~16% for the 50 cm target radius.

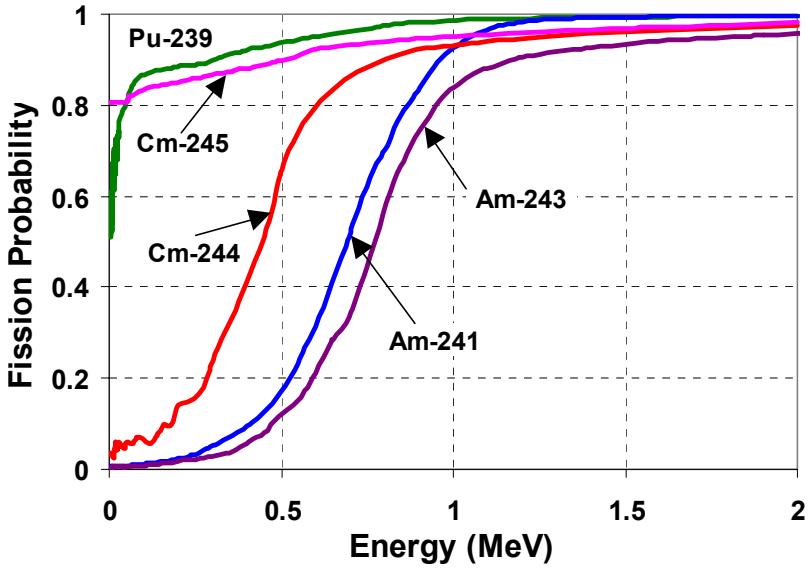

Fig. 3. Fission cross-section over absorption cross-section for ^{239}Pu, ^{241}Am, ^{243}Am, ^{244}Cm and ^{245}Cm (ENDF/B-VI.7) [11].

Table 3 Fraction of neutrons leaking out radially from the target that have energy below 1 MeV

Target Radius (cm)	E < 1 MeV (%)
10	38.4
20	55.2
30	69.1
40	79.3
50	86.4

3.2 Comparison of the CEM Model with the Bertini Model

In our previous studies of the proton source efficiency [4, 10], the physics models used in the MCNPX simulations was the Bertini package (default in MCNPX). However, the Bertini model has shown some disagreements with experimental results [12], the main deficiency of the model being that it over-predicts the low-energy neutron production resulting from high-energy protons impinging on different heavy-metal targets. With the purpose of improving the agreement with experiments [13], the Bertini package has in this study been replaced by the CEM package.

3.2.1 Primary Spallation Neutrons

In order to study the differences between the Bertini model and the CEM model, simulations determining the primary spallation neutron production, i.e. the number of neutrons produced in an average single spallation reaction, have been performed. The primary neutrons were defined as the neutrons created in a proton-induced spallation reaction and in order to record the collection of the these neutrons, the trajectory of a neutron was immediately terminated and its properties recorded at the moment it first appeared in the MCNPX transport simulation.

In Fig. 4, the energy spectrum of the primary spallation neutrons created using the Bertini model and the CEM model are plotted and the expected result that the Bertini model yields a higher number of neutrons in the low-energy range (below ~15 MeV) than the CEM model is clearly seen. In the energy range between about 15 and 80 MeV, the situation is slightly the opposite, while above this energy the neutron production is similar for the two models. Altogether, the number of primary spallation neutrons created for each proton (Z_{prim}) using the Bertini model was 15.0, while only 11.9 using the CEM model.

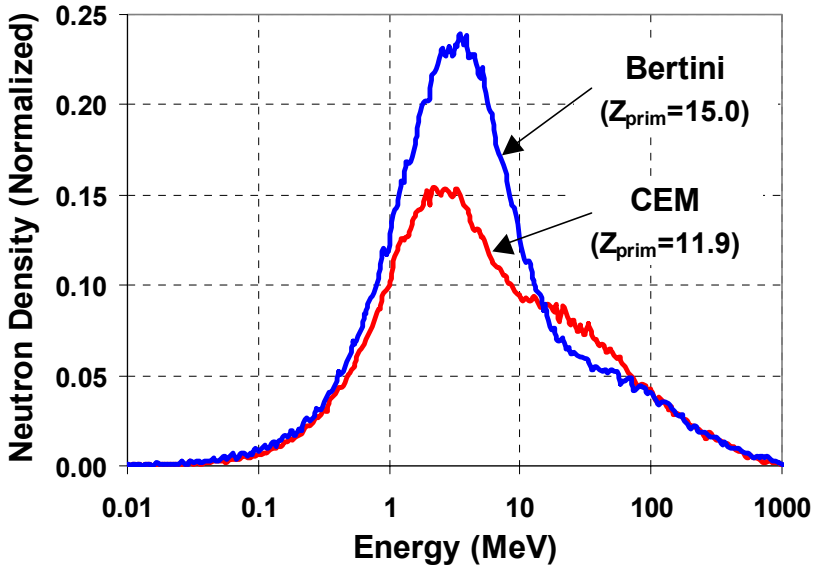

Fig. 4. Energy spectrum of the primary spallation neutrons (the neutrons created in an average spallation reaction) induced by 1000 MeV protons impinging on a Pb-Bi nucleus. Z_{prim} is the number of primary spallation neutrons created for each proton.

3.2.2 Target Leakage Neutrons

In the following study, the 1000 MeV protons were accelerated towards the spallation target of a radius varying from 10 to 50 cm, and the neutrons leaking out from the target were studied using the two different high-energy physics models. It is seen in Table 4 that the number of target leakage neutrons created for each source proton (Z_{tot}) increases for increasing target radius, which is due to the multiplication, by (n,xn)-reactions and secondary spallation reactions, of the primary spallation neutrons carrying very high energy. In column 3 and 5 in Table 4, the number of secondary neutrons (the neutrons created in reactions induced by the primary neutrons, $Z_{sec} = Z_{tot} - Z_{prim}$) is listed and it is seen that those numbers are more or less the same for all target radii, independently of which physics model that is used. This indicates that only the high-energy primary neutrons, which are approximately equal in number for the two different models, contribute to the production of secondary neutrons. This assumption can further be explained by the fact that (n,xn)-reactions in lead and bismuth have an energy threshold at about 7 MeV. The primary spallation neutrons with energy below 7 MeV (10.2 and 7.2 neutrons per proton, respectively, from using the Bertini and the CEM model) are thus transported through the target without inducing any multiplicative reactions. The primary neutrons with energy higher than this threshold (~4.7 for both physics models), on the other hand, are multiplied on their way out through the lead-bismuth and, consequently, the number of created secondary neutrons gradually increases with increasing target radius. However, as the target radius grows larger and reaches a value in the order of 40 cm, the fraction of neutrons above the threshold energy at 7 MeV is only about 1.5%, which is the reason why Z_{sec} (and Z_{tot}) changes only slightly when the radius increases from 40 to 50 cm.

Table 4 Number of primary neutrons (Z_{prim}), secondary neutrons (Z_{sec}) and total number of neutrons created in the target (Z_{tot}) for each incident 1000 MeV proton, calculated by MCNPX using the Bertini and the CEM physics packages.

	Bertini		CEM	
Z_{prim}	15.0		11.9	
Target Radius (cm)	Z_{tot}	Z_{sec}	Z_{tot}	Z_{sec}
10	21.9	6.9	18.7	6.8
20	26.8	11.8	23.6	11.7
30	29.1	14.1	25.9	14.0
40	30.1	15.1	27.0	15.1
50	30.3	15.3	27.3	15.4

Z_{prim} is the number of primary spallation neutrons per incident proton, i.e. the neutrons created in an average spallation interaction.
Z_{sec} is the number of secondary neutrons per incident proton, i.e. the neutrons created in reactions induced by the primary spallation neutrons.
Z_{tot} is the total number of neutrons created in the target per incident proton ($Z_{tot} = Z_{prim} + Z_{sec}$).

3.2.3 Proton Source Efficiency

The effect on the proton source efficiency by exchanging the two physics models in the MCNPX simulations is somewhat similar to that on the neutron production in the target. The results obtained show that replacing the Bertini model by the CEM model decreases ψ^* by approximately 11% to 9%, these numbers corresponding to the target radii of 10 cm and 50 cm, respectively. The reason why these relative differences are smaller than the corresponding

ones for Z_{tot} (15% to 10%) is that the high-energy parts of the target neutron leakage spectra, which has the strongest impact on ψ^*, are very similar for the two different models.

4 Conclusions

In order to study the optimization of the proton beam power amplification (core power divided by proton beam power) in an ADS, the proton source efficiency (ψ^*) has been investigated for a homogeneous and a heterogeneous distribution of Am and Cm. The results from the MCNPX simulations show that moving Cm to the inner part of the active core in the heterogeneous configuration increases ψ^*, compared to the homogeneous configuration, where the minor actinides are mixed with each other. This difference is due to the fact that Cm has higher fission probability than Am for neutrons below about 1.0 MeV, which enhances the multiplication of the neutrons entering into the fuel and thus increases ψ^*. The gain in choosing the heterogeneous Cm distribution is most important for large target radii, since the fraction of target leakage neutrons below 1 MeV is an increasing function of target radius. For the 10 cm target radius, the relative difference in ψ^* between the two configurations was found to be 5%, whereas as much as 16% for the 50 cm target radius.

Comparing the effects on neutron production in the target and on ψ^* by using two different physics packages provided by MCNPX, the Bertini model and the CEM model, the following findings were obtained. First, the Bertini model produces a larger number of primary spallation neutrons than does the CEM model (15.0 compared to 11.9), the major part of the difference being found in the low-energy part of the spectrum (below ~15 MeV). Consequently, the total number of neutrons produced in the target for each source proton is also higher for the Bertini model, the difference being about 3 neutrons for all target radii. The reason why the difference is constant and not dependant on target radius is that the production of high-energy primary spallation neutrons, that are responsible for the secondary neutron multiplication in the target, is about the same for the two models. Finally, concerning the proton source efficiency, the ψ^*-values obtained for the Bertini model were found to be larger by about 10% than those obtained for the CEM model.

Acknowledgements

This work was financially supported by the Swedish Centre for Nuclear Technology, SKB AB (Swedish Nuclear Fuel and Waste Management Co) and the European Commission (Project MUSE: FIKW-CT-2000-00063).

References

1 M. Salvatores et al., ”Long-Lived Radioactive Waste Transmutation and the Role of Accelerator Driven (Hybrid) Systems,” *Nucl. Instrum. Methods A*, **414**, 5 (1997).

2 D. G. Foster et al., ”Review of PNL Study on Transmutation Processing of High Level Waste,” LA-UR-74-74, Los Alamos National Laboratory (1974).

3 T. Takizuka et al., “Conceptual Design of Transmutation Plant,” Proc. Specialist Mtg. Accelerator Driven Transmutation Technology for Radwaste, LA-12205-C, p. 707, Los Alamos National Laboratory (1991).

4 P. Seltborg et al., “Definition and Application of Proton Source Efficiency in Accelerator Driven Systems,” *Nucl. Sci. Eng.*, **145**, 390 (2003).

5 G. ALIBERTI et al., "Analysis of the MUSE-3 Subcritical Experiment", Int. Conf. Global 2001, France, Paris, September (2001).

6 L. S. WATERS, "MCNPX™ User´s Manual – Version 2.1.5," Los Alamos National Laboratory, November 14, (1999).

7 H. W. BERTINI, Phys. Rev. **131**, 1801 (1969).

8 S. G. Mashnik and A. J. Sierk, "Improved cascade-exciton model of nuclear reactions," Proc. SARE4, September 14–16, 1998, Knoxville, TN, USA (ORNL, USA, 1999) pp. 29–51; Eprint nucl-th/9812069.

9 OECD Nuclear Energy Agency, "Accelerator-driven Systems (ADS) and Fast Reactors (FR) in Advanced Nuclear Fuel Cycles; A Comparative Study", Paris, France, (2002).

10 P. Seltborg and J. Wallenius, "Proton Source Efficiency for different Inert Matrix Fuels in Accelerator Driven Systems," Int. Meeting AccApp'03, June 1-5, 2003, San Diego, California, USA (2003).

11 NEA homepage, http://www.nea.fr/janis/

12 S. LERAY et al., "Spallation Neutron Production by 0.8, 1.2, and 1.6 GeV Protons on various Targets," *Phys. Rev*., **C65** (2002).

13 S. G. Mashnik and A. J. Sierk, "Recent Developments of the Cascade-Exciton Model of Nuclear Reactions", Int. Conf. on Nucl. Data for Science and Technology, October 7-12, 2001, Tsukuba, Japan, LA-UR-01-5390 (2001).